BIOCHEMISTRY
including biophysical chemistry & molecular biology

Current Topic

pubs.acs.org/biochemistry

Glycines: Role in α-Helical Membrane Protein Structures and a Potential Indicator of Native Conformation

Hao Dong,[†,‡] Mukesh Sharma,[§,∥] Huan-Xiang Zhou,[†,‡] and Timothy A. Cross*[,†,§,∥]

[†]Institute of Molecular Biophysics, Florida State University, Tallahassee, Florida 32306, United States

[‡]Department of Physics, Florida State University, Tallahassee, Florida 32306, United States

[§]Department of Chemistry and Biochemistry, Florida State University, Tallahassee, Florida 32306, United States

[∥]National High Magnetic Field Laboratory, Florida State University, Tallahassee, Florida 32306, United States

Supporting Information

ABSTRACT: Among the growing number of membrane protein structures in the Protein Data Bank, there are many transmembrane domains that appear to be native-like; at the same time, there are others that appear to have less than complete native-like character. Hence, there is an increasing need for validation tools that distinguish native-like from non-native-like structures. Membrane mimetics used in protein structural characterizations differ in numerous physicochemical properties from native membranes and provide many opportunities for introducing non-native-like features into membrane protein structures. One possible approach for validating membrane protein structures is based on the use of glycine residues in transmembrane domains. Here, we have reviewed the membrane protein structure database and identified a set of benchmark proteins that appear to be native-like. In these structures, conserved glycine residues rarely face the lipid interstices, and many of them participate in close helix−helix packing. Glycine-based validation allowed the identification of non-native-like features in several membrane proteins and also shows the potential for verifying the native-like character for numerous other membrane protein structures.

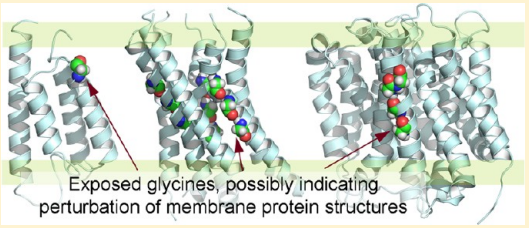

α-Helical membrane protein structures can be influenced by the membrane mimetic environments in subtle and not so subtle ways.[1−6] Anfinsen in 1973[7] stated "that the native conformation (of a protein) is determined by the totality of interatomic interactions and hence by the amino acid sequence in a given environment." Therefore, the interactions from the heterogeneous membrane environment contribute to the sum of interactions responsible for defining the three-dimensional structure of a membrane protein. Here, we focus on the influence of the physical properties of membrane environments instead of the influence of specific lipids. Recently, a detailed description of how promiscuous membrane proteins can be in their interactions with different lipids has been published.[8] A challenge for membrane protein structural biologists is to mimic the membrane environment adequately to stabilize the native protein structure, while preparing a sample that is appropriate for the specific structural technique. Only bacteriorhodopsin has been characterized in its native membrane environment.[9] A few others have been characterized in liquid crystalline lipid bilayers[4,10−14] and more in the presence of lipids.[15−17] The vast majority have been characterized in the presence of detergents, most in crystal lattices and others in detergent micelles. As the number of α-helical membrane protein structures increase in the Protein Data Bank (PDB), there is an increasing need for tools to evaluate their native-like structural quality. Here, we explore the basis for developing a tool to test the compatibility of membrane protein structures with a native membrane environment.

Large membrane proteins with cofactors in the transmembrane (TM) domains may have significant interactions with these cofactors to stabilize tertiary structures.[18−20] However, the tertiary stability of a TM domain with only a few helices is often limited by very weak interhelical interactions, because of a largely hydrophobic amino acid composition and the tendency for TM helices to have uniform backbone torsion angles resulting from strong hydrogen bonding in the low-dielectric membrane environment.[21−24] In other words, the packing of a set of relatively rigid and uniform helical rods generates marginal tertiary stability. This minimal stability permits membrane proteins to adopt multiple tertiary conformations with different helical packing for various functional states. Consequently, there is a tendency to justify structural variations among different characterizations of a protein as reflecting different functional states. However, each of these structures should be compatible with the native membrane environment, and therefore, the native-like character of these structures should be critically assessed, especially because TM domains with marginal tertiary stability are subject to distortion by membrane mimetics.[1−4,10]

Received: October 26, 2011
Revised: May 31, 2012
Published: May 31, 2012

   dx.doi.org/10.1021/bi300090x | *Biochemistry* 2012, 51, 4779−4789

Although membrane protein structural biologists have used functional assays to validate their structural conclusions, often these assays have to be performed in an environment different from that used for structural characterization, such as the assays for ion channel conductance, where a bilayer is needed. These assays validate the protein constructs, but not the structures. These assays are important in that they validate the non-native protein constructs often used for structural characterization. Site-directed mutagenesis, binding of antibodies, deletion of loops and termini, and insertion of water-soluble proteins into loops have frequently been used for recent structural characterizations,[25−28] yet in addition to the functional viability of the construct, it is important to validate the structure obtained from a membrane mimetic environment with regard to whether it is consistent with the native membrane environment. Functional misunderstanding of proteins influenced by the membrane mimetic environment can be propagated through the literature for many years.[3,24,29−31]

Several approaches have been used to obtain detailed structural data for membrane proteins within a lipid environment and even a cellular membrane environment. Electron crystallography (32 depositions in the PDB) has been used to characterize multiple membrane proteins in a lipid environment matrix.[17,32−35] Solid state NMR spectroscopy (52 depositions in the PDB) has been used to obtain structural restraints for membrane proteins in liposomal or planar bilayer environments.[4,10−14] Other techniques such as ESR have also provided important structural restraints for membrane proteins in proteoliposomes. Such data can be of great use in validating membrane protein structure, because these lipid environments are more native-like than the detergent environments typically used by X-ray crystallography and solution NMR spectroscopy that have determined the majority of the membrane protein structures in the PDB.

It is well recognized that charged and perhaps polar residues when exposed to the hydrophobic interstices of lipid bilayers will result in a significant energetic penalty that has to be compensated to achieve a stable structure.[36,37] Indeed, viewing the charged residues of a membrane protein is a useful way for evaluating the native-like quality of the structure. While polar residues like serine and threonine can form intrahelical hydrogen bonds to backbone amides and thereby shield both the polar side chains and the polar backbone from the hydrophobic environment,[38] even these polar residues have a tendency to avoid the lipid interstices.[39] Other, hydrophilic residues are rarely exposed to the fatty acyl chains in a membrane environment.

Here, we suggest another approach for validating the native-like character of membrane protein structures, based on the location of glycine residues, that is complementary to approaches based on the charged and polar residues.

INFLUENCE OF MEMBRANE MIMETIC ENVIRONMENTS

There are many ways that membrane mimetic environments can influence membrane protein structures and, conversely, for membrane proteins to influence the membrane mimetic environments. Synthetic bilayers used for solid state NMR, ESR, and electron crystallographic studies may have a hydrophobic mismatch with membrane proteins,[40−42] a lack of bilayer asymmetry, chemical and electrical gradients, lipid heterogeneity, or curvature frustration,[43,44] and a nonnative lateral pressure profile.[45] Nevertheless, synthetic bilayers are significantly better than other membrane mimetics. Detergent micelles provide a single highly curved hydrophilic surface that generates a different environment for amphipathic helices that bind at the lipid hydrophobic−hydrophilic interface.[46] This hydrophilic surface can stabilize a distorted helical structure, by solvating hydrophilic residues in the middle of a curved helix. Moreover, the hydrophobic dimension of a detergent micelle can be easily changed in response to optimal packing of the helices that is potentially different from that in the native membrane.[2]

Detergents also generate a weaker hydrophobic environment compared with lipid bilayers, with extensive penetration of water into the micelle[35,47−49] as well as a weaker and distorted lateral pressure profile.[45,50] While lipid headgroups retain considerable dynamics, the lateral pressure profile in membranes suggests close packing of the lipid headgroups and/or glycerol backbone around membrane-solubilized proteins. In detergent micelles, the headgroup region is even more dynamic because of the high curvature of the hydrophilic surface and consequently the lateral pressure profile is less dramatic and the headgroup region less tightly packed.[3] In crystal environments, contacts between proteins within and between the unit cells can distort the protein structure. Hydrophilic organics and water molecules are often embedded in what would be the very low dielectric environment of the membrane interstices, thereby weakening the hydrophobic environment. Also, in crystal lattices, detergents often appear to form a thin hydrophobic layer for membrane proteins. Consequently, if a membrane protein is dependent on its environment for defining the hydrophobic thickness, the structure may be distorted in such a crystalline environment.

Detergents also have a monomeric concentration that is $\geq$6 orders of magnitude higher than that for monomeric lipids.[51] As a result, water-soluble and/or dynamic domains as well as pores through the membrane protein structure may be altered when detergents are used as a membrane mimetic,[2,52] because of the relatively high concentration of monomeric detergents in the bulk aqueous environment. Thus, membrane mimetics provide many opportunities for introducing non-native-like structural perturbations.

NON-NATIVE-LIKE STRUCTURAL PERTURBATIONS

The need for validation tools is apparent on many different levels. The observed structural influences of membrane mimetics can be minor, such as charged side chains that are oriented toward what would be the bilayer interstices instead of toward the aqueous environment, or nearly complete disruption of the tertiary structure as in the voltage-sensing domain of the well-known initial structure of KvAP (PDB entry 1ORQ).[26] Between those possibilities, there are multiple examples of TM domains that appear to have less than complete native-like character. This is not to say that these structures are not significant stepping stones toward the structural and functional understanding of these proteins, but if the non-native-like structural perturbations are unrecognized these structures can also be misleading.

In a few cases, there are multiple structures of the same or similar membrane protein obtained under differing conditions that provide possible insights into the structural abnormalities. Because of the potential for multiple functional conformations, care must be taken in such interpretations. Therefore, the goal here is not so much to validate these TM domains as representing functional states but rather to validate these

structures as being compatible with native membrane environments. While being heterogeneous, these environments still have well-defined properties, such as a very low dielectric constant in the hydrophobic interior and a significant hydrophobic dimension.

Potential non-native-like features are illustrated by three structures in Figure 1. KdpD is a histidine kinase receptor for regulating the operon that encodes the K^+ transporter, Kdp. The solution NMR structure (2KSF) of the TM domain of KdpD is a four-helix bundle in detergent micelles[53] (Figure 1a). A striking feature of these helices is that two of them, helices 2 and 3, are not nearly long enough to span the approximate 30 Å hydrophobic dimension of the native membrane, suggesting that the hydrophobic span of the membrane mimetic is insufficient. Throughout much of helices 1, 3, and 4, there is hydrogen−deuterium exchange in the amide backbone, suggesting exposure to water and consequently a weak hydrophobic environment. In addition, numerous hydrophilic side chains (Ser409, Thr413, Ser448, Thr452, and Asn493) are exposed to what would be the lipid interstices as opposed to being oriented toward the interior of the helical bundle. Indeed, it appears as if there is a minimal number of hydrophilic side chains oriented toward the interior of the bundle.

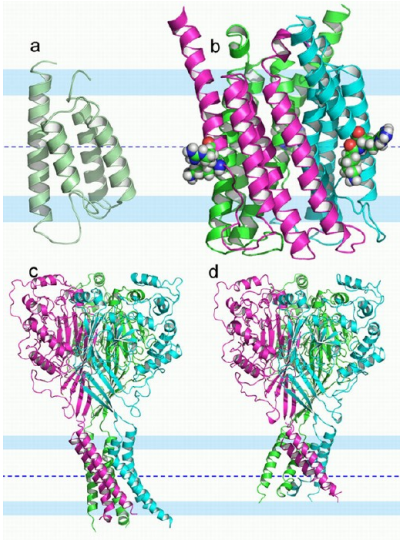

Figure 1. Putative non-native-like structural perturbations of three membrane proteins. The membrane central plane was located as described in Supporting Information. This membrane central plane is shown as a blue dashed line; interfacial regions are represented by 8 Å wide pale blue colored bands, and the conservative hydrophobic thickness between them is 25 Å. (a) Histidine kinase receptor KdpD TM domain (solution NMR structure, PDB entry 2KSF). This four-helix bundle has two very short helices and multiple hydrophilic residues exposed to the hydrophobic region of the would-be membrane. The short helices dictate that hydrophilic backbone amides of the interhelical loops are also exposed to the membrane interstices. (b) 5-Lipoxygenase-activating protein (4.0 Å resolution structure, PDB entry 2Q7M). The three chains are displayed in different colors. Helix 4 appears to be shifted along the helical axis, exposing two charged residues (Lys116 and Arg117 in space filling mode with carbon atoms colored green, nitrogen atoms blue, oxygen atoms red, and hydrogen atoms white) to the very center of the membrane, and the interhelical loop between helices 3 and 4 is drawn into the lipid interstices exposing more hydrophilic sites to the hydrophobic region of the membrane. (c and d) Two structures of the trimeric acid-sensing ion channel [1.9 Å resolution structure, PDB entry 2QTS (c); 3 Å resolution structure, PDB entry 3HGC (d)]. They have similar symmetric extramembranous domains but different TM domains. The TM domain in panel c has a sufficient hydrophobic dimension but is asymmetric, probably the result of substantial crystal contacts, while the TM domain in panel d is more symmetric but does not span the hydrophobic dimension of native membranes.

Trimeric 5-lipoxygenase-activating protein (FLAP) has four TM helices per monomer. FLAP (Figure 1b) has been characterized by X-ray crystallography (PDB entry 2Q7M), showing both Lys116 and Arg117 in what would be the middle of the hydrophobic region.[54] Both the guanidinium group of Arg117 and the backbone amide of Phe138 form electrostatic contacts with a neighboring trimer in the crystal. As a result, helix 4 (including Lys116 and Arg117 residues) appears to be shifted along the direction of the helical axis to the extent that the interhelical loop (residues 108−115) extends to the center of what would be the membrane, exposing a large number of hydrophilic amides to the hydrophobic environment of the would-be membrane interior. Moreover, the C-terminal residues (138−149) of the neighboring trimer have their amides completely exposed to the would-be membrane interior surrounding the first trimer. Another member of this protein family, microsomal prostaglandin E synthase 1, has been characterized in a lipid environment by electron crystallography (PDB entry 3DWW) and shows four complete TM helices with no exposure of charged residues or amides from nonhelical segments exposed to the fatty acyl chains of the lipid environment.[55]

There are two crystal structures of the acid-sensing ion channel (ASIC) using somewhat different constructs.[56,57] These structures are also trimers with each monomer contributing a pair of TM helices. The very large symmetric extracellular domains from the two structures superimpose well, but while the TM domain of the 2009 structure has approximate 3-fold symmetry (Figure 1d), the 2007 structure lacks this symmetry (Figure 1c), possibly because of substantial crystal packing interactions. This latter structure has long helices that would readily span the membrane, while the 2009 structure has a very short hydrophobic dimension resulting from helices that are both kinked and tilted at an overly large angle to the symmetry axis. The result is that the 2009 structure is not consistent with the hydrophobic dimension of native membranes and the 2007 structure deviates from the expected 3-fold symmetry.

GLYCINE RESIDUES IN TRANSMEMBRANE HELICES

Glycine and proline residues are surprisingly common in TM α-helices,[24,58] even though these residues are known to be helix-destabilizing in water-soluble proteins.[59−62] There have been several reasons identified for their presence in TM helices. In the TM environment, helical hydrogen bonds are stronger because of the low dielectric of this environment.[21−23,63] The resulting helical regularity would limit helix packing opportunities, and hence glycine (having access to a much greater ϕ and ψ torsional space) and proline (lacking an amide proton for hydrogen bonding within the helix) are present to induce kinks. These two residues, although destabilizing the helical structure, permit enhanced tertiary structural interactions from an increased surface area between helices and hence enhanced tertiary structural stability that would otherwise be very limited.[20]

dx.doi.org/10.1021/bi300090x | *Biochemistry* 2012, 51, 4779−4789

Table 1. Benchmark Set of 26 Membrane Proteins

	PDB entry	resolution or method	name	oligomeric state
a	1FX8	2.2 Å	*Escherichia coli* glycerol facilitator	tetramer
b	1L7V	3.2 Å	*E. coli* vitamin B12 ABC transporter	dimer
c	1P7B	3.65 Å	potassium channel KirBac1.1	tetramer
d	2A65	1.65 Å	bacterial homologue of Na^+/Cl^--dependent neurotransmitter transporter	dimer
e	3ND0	3.5 Å	cyanobacterial HCl exchange antiporter	dimer
f	2AHY	2.4 Å	*Bacillus cereus* NaK channel	tetramer
g	2EI4	2.1 Å	archaerhodopsin-2	tetramer
h	2GIF	2.9 Å	*E. coli* multidrug efflux transporter AcrB	trimer
i	2J7A	2.3 Å	cytochrome *c* quinol dehydrogenase	dimer
j	2L0J	solid state NMR	influenza A M2 proton channel	tetramer
k	2KYV	solid state/solution NMR	phospholamban	pentamer
l	2NS1	1.96 Å	*E. coli* GlnK-bound ammonia channel	trimer
m	3DQB	3.2 Å	G-protein peptide-bound G-protein-coupled receptor opsin	dimer
n	3DWW	electron crystallography	glutathione-bound microsomal prostaglandin E synthase 1	trimer
o	3EAM	2.9 Å	*Gloeobacter violaceus* ligand-gated ion channel	pentamer
p	3NCY	3.2 Å	arginine agmatine antiporter	dimer
q	2YVX	3.5 Å	*Thermus thermophilus* magnesium transporter	dimer
r	2ONK	3.1 Å	ModA-bound *Archaeoglobus fulgidus* molybdate ABC transporter	dimer
s	2R9R	2.4 Å	chimera Kv2.1 and Kv1.2 potassium channel	tetramer
t	2OAR	3.5 Å	*Mycobacterium tuberculosis* large mechanosensitive channel	pentamer
u	3HD6	2.1 Å	*Homo sapiens* ammonium transporter Rh type C	trimer
v	3O7Q	3.1 Å	*E. coli* fucose transporter	monomer
w	3MKT	3.65 Å	*Vibrio cholera* multidrug and toxic compound extrusion transporter	monomer
x	3M71	1.2 Å	*Haemophilus influenzae* SLAC1 channel	trimer
y	2BL2	2.1 Å	*Enterococcus hirae* V-type Na^+-ATPase rotor	decamer
z	2ZW3	3.5 Å	*H. sapiens* connexin-26 gap junction channel	hexamer

During functional processes, membrane proteins frequently undergo significant structural rearrangement involving kinking and repacking of helices.[64,65] The presence of glycine and proline residues can facilitate such rearrangements. Indeed, TM helices can be remarkably regular even in the presence of these residues, leading to the moniker that these residues can be pro-kink sites; i.e., they induce kinks in some functional states and not in others.[23] Kinks also lead to exposure of amide hydrogen bonding sites for structural or functional purposes. Such exposure is needed, because there are few hydrophilic side chains that can provide chemically active sites, and hence, the backbone is a very important source for functional activity, for instance, in the solvation of ions in the gramicidin A channel and in the KcsA channel.[11,66] The exposure of backbone amides through helix kinks may also lead to the binding of water in the bilayer interstices where its presence is very limited. Water is known to play important roles in TM domains, including the facilitation of structural interconversion through hydrogen bond rearrangements[65,67,68] and proton wires;[69,70] the exposure of backbone amides through kinks could greatly enhance these functional activities.

Moreover, glycine residues are known to be important for helix packing by allowing close approach of the helical backbones.[71] The pioneering studies of glycophorin identified GxxxG motifs that permitted close packing of a dimer and increased helix−helix stability associated with an increased number of van der Waals contacts,[20,72] an increased number of long-range electrostatic interactions between helices, and the potential for C_α−H hydrogen bonding.[63,73] Since then, GxxxG motifs and permutations involving alanine, serine, and threonine have been widely identified.[74−77] In addition, glycine zippers (GxxxGxxxG) have been described for helices that pack with a modest crossing angle.[78]

This extensive use of glycine in TM helices could facilitate β-strand formation, but the frequent presence of proline residues would counter this tendency toward the formation of β-strands,[77,79,80] resulting in the assurance that TM helices are formed despite the extensive use of glycine. Consequently, it would seem that glycine is used judiciously for facilitating tertiary and quaternary structural stability.

A BENCHMARK OF NATIVE-LIKE STRUCTURES

Using two criteria, an adequate hydrophobic dimension for spanning the hydrophobic dimension of the bilayer and a lack of exposure of the hydrophilic site to what would be the interstices of native membranes, an initial set of benchmark proteins from the PDB were identified. From these proteins, we extracted distributions and rules that are expected to be followed by native-like structures. Structures that deviate from these norms can then be suggested to contain non-native-like features.

The 26 proteins comprising our benchmark are listed in Table 1 and displayed in Figure 2. These structures span many of the structure−function families identified for TM helical proteins on the "Membrane Proteins of Known 3D Structure" website (http://blanco.biomol.uci.edu/mpstruc/listAll/list). In identifying structures for our benchmark set, we did not include any with multiple cofactors stabilizing the TM domains as these cofactors contribute significantly to structural stability. For the remaining structure−function families, nearly half are represented in our benchmark set. We have considerable confidence that these and many other proteins from the same structure−function families have native-like structures. (Many structures from the other structure−function families may also be native-like, but we have chosen conservatively so that the statistics of native-like structures are not distorted.) None of the bench-

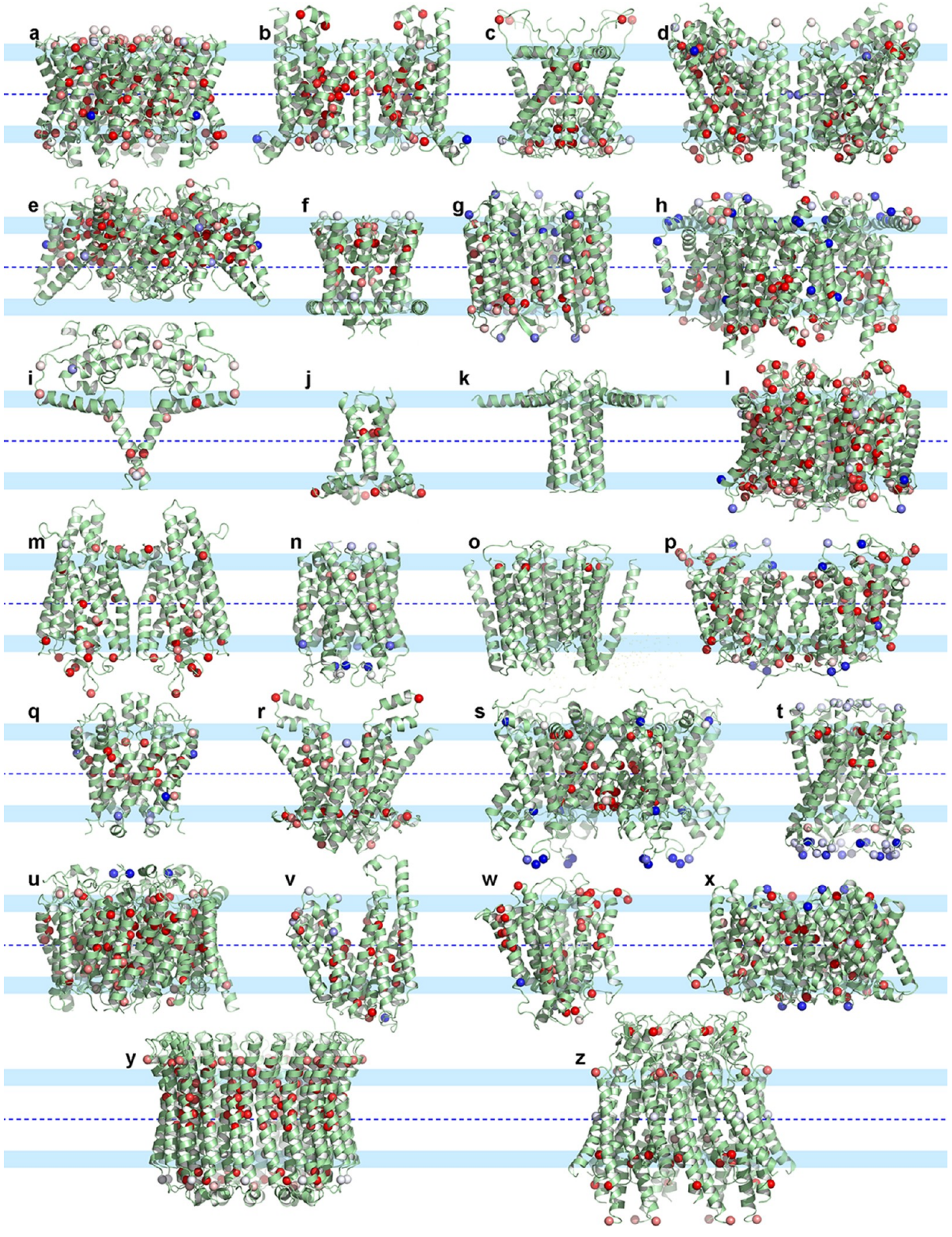

Figure 2. Transmembrane domains of benchmark membrane protein structures. C_α atoms of glycines are shown as spheres and color-coded according to their conservation scores [red for highly conserved, blue for not conserved, and pale colors for intermediate (see the Supporting Information for details)]. Default parameters for residue conservation were used for all the proteins except for the ligand-gated ion channel (PDB entry 3EAM), where the minimal sequence identity for sequence alignment was lowered from the default (35%) to 25%. (a–z) Structures corresponding to entries a–z, respectively, in Table 1. Note that the outward-facing surface of the helices in these proteins is rarely interrupted by a glycine sphere.

dx.doi.org/10.1021/bi300090x | *Biochemistry* 2012, 51, 4779–4789

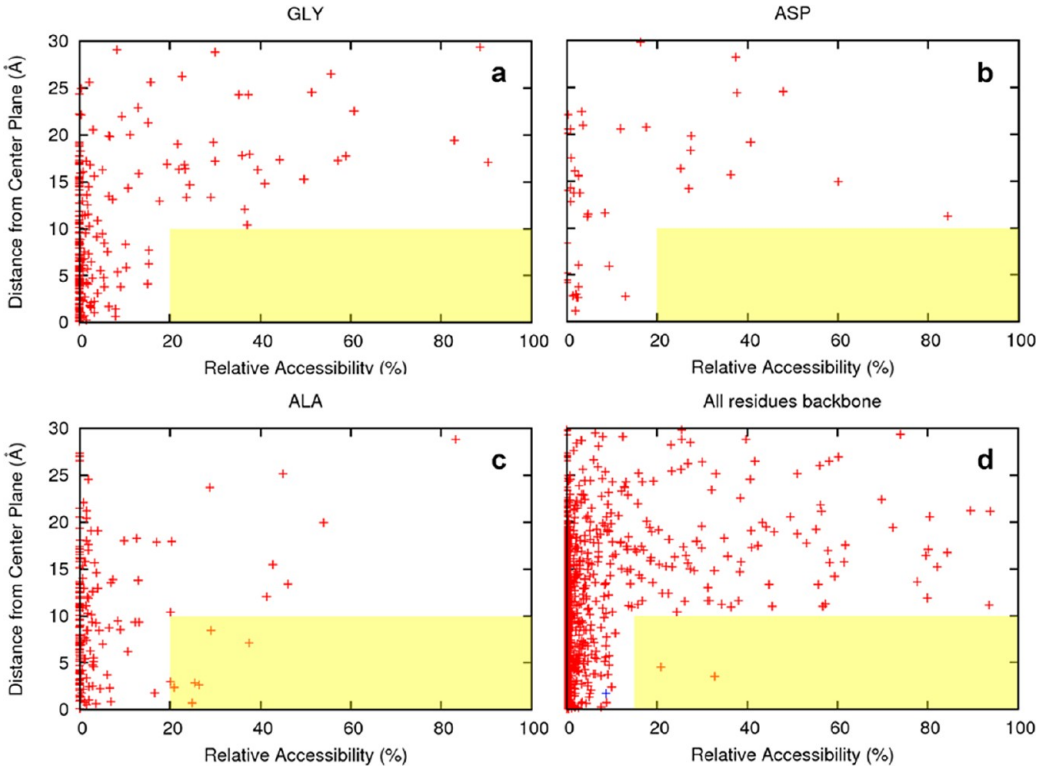

Figure 3. Scatter plots displaying relative accessibility and distance (expressed as |*z*|, i.e., the absolute value of *z*) from the membrane central plane for the conserved residues in the benchmark proteins. Relative accessibility [i.e., the percentage of the nominal maximal area (irrespective of secondary structure) (see the Supporting Information)] was calculated for either a whole residue or for the backbone polar atoms (C, O, and N) only. Oligomeric protein structures were used to calculate the solvent accessibility of each residue. However, for each oligomeric protein, only a single chain was used to count the number of glycines and other residues as well as for the backbone statistics. (a−c) Whole-residue relative accessibility for glycine, aspartate, and alanine residues. The hydrophobic region was conservatively defined as the region 10 Å from the bilayer center. Surface exposure above 20% was considered significant. (d) Backbone relative accessibility for all 20 types of residues. Lipid-facing surface exposure of the backbone above 15% was considered significant. The two backbone sites in the entire benchmark set that have significant exposure are both proline residues (Pro315 of the B12 ABC transporter, PDB entry 1LV7, and Pro300 of a ligand-gated channel, PDB entry 3EAM). The glycine residue with the greatest level of exposure (Gly87 of the NaK channel, PDB entry 2AHY) is highlighted as a blue plus.

mark structures have charged residues in the hydrophobic interstices, and they all have helices that appear to span a hydrophobic dimension consistent with native membrane environments. These proteins range in size from the solid state NMR structure of the tetrameric conductance domain (PDB entry 2L0J) of the influenza A M2 protein with a single TM helix per monomer,[10] and the X-ray crystallographic structure of dimeric cytochrome *c* quinol dehydrogenase (PDB entry 2J7A) also with a single TM helix per monomer,[81] to the crystallographic structure of the dimeric HCL exchange transporter (PDB entry 3ND0).[82]

CONSERVED GLYCINES AND THEIR STRUCTURAL ROLES

The 26 benchmark proteins have a total of 673 glycines, compared to 837 alanines and 244 aspartates. Below we contrast these residues in terms of sequence conservation, solvent accessibility, and distance (*z*) from the would-be bilayer center (presented as the absolute value, |*z*|). The bilayer center was defined (see the Supporting Information) on the basis of the distribution of the C_α atoms of charged residues in each protein and could have a significant error. As a result, the hydrophobic region of the bilayer was conservatively limited to the region 10 Å from the bilayer center for evaluating the characteristics of glycine residues. Sequence conservation scores were obtained from the ConSurf web server;[83] we refer to residues with the top 20% of the conservation scores as being conserved.

Of the 673 glycines, 264 (39%) reside in the hydrophobic region, illustrating just how common glycine residues are in TM helices. In comparison, 40% of the alanines but only 8% of the aspartates have |*z*| values of <10 Å. Glycine thus has a tendency to be located in the hydrophobic region similar to that of alanine, while aspartate avoids the hydrophobic region of the bilayer. Therefore, on the basis of this sampling, glycine, despite the nearly lowest helical propensity (proline is the only residue with a lower propensity), has the same likelihood of being in a TM helix as alanine, the residue with the highest helix propensity.[61]

Of the 264 glycines in the hydrophobic region of the bilayer, 147 (56%) are conserved; in contrast, only 31% of the glycines outside the hydrophobic region are conserved. For the alanines, 29% are conserved in the hydrophobic region and 19% are conserved outside the hydrophobic region. There are too few aspartates with |*z*| values of <10 Å to contrast the two regions in terms of conservation, but overall, 75% of these residues are conserved. The fact that a very high fraction of the glycines are conserved further confirms that the glycines have important roles in these helices, as described above. Indeed, without a good reason to be present, and hence conserved, one might expect an evolutionary pressure to remove these glycine residues, because they destabilize helical structures.

dx.doi.org/10.1021/bi300090x | *Biochemistry* 2012, 51, 4779−4789

In Figure 3a–c, we present scatter plots for the conserved glycines, alanines, and aspartates showing their whole-residue (i.e., including the side chains) relative accessibility as a function of |z| value. Surprisingly, in the hydrophobic region (i.e., |z| < 10 Å), the glycines are similar to the aspartates in avoiding exposure to the lipid fatty acyl chains. No residues of either type have >20% accessibility to the hydrophobic interstices of the bilayer. In comparison, 4% of the alanines in the hydrophobic region have >20% accessibility to the hydrophobic interstices. Here 20% was used as the threshold in whole-residue relative accessibility for considering a residue to be exposed. As a reference, residues in ideal poly-Gly, poly-Asp, and poly-Ala helices would have 64, 66, and 59% whole-residue exposure, respectively.

Glycine thus exhibits a strong tendency to avoid exposure to the hydrophobic interstices of the bilayer. While the exact numbers for accessibility may be subject to variation because of calculation details (e.g., the nominal maximal areas used for calculating relative accessibility and the value, 20%, used here as the accessibility threshold for considering a residue as exposed), the avoidance of exposure for glycine is unmistakable. This is likely driven by two factors: the inability of glycine residues to perform their function (summarized above as promoting tertiary structure) while exposed to the hydrophobic environment and the need to avoid exposure of hydrophilic backbone atoms (N, C, and O) to the hydrophobic environment. Whereas glycines in an ideal poly-Gly helix have as much as 31% backbone exposure, Figure 3d shows that, in the hydrophobic region (i.e., |z| < 10 Å) the greatest level of exposure of the backbone by any glycine residue in our benchmark set is only 9%. Furthermore, all hydrophilic backbone atoms, regardless of side chain type, are well shielded from the hydrophobic interstices of the bilayer; all but two residues (two prolines) have ≤15% accessibility. While other types of residues can rely on side chains to partially shield their hydrophilic backbone atoms (backbone exposure is down from 31% in a poly-Gly helix to 15% in a poly-Ala helix and to only 2% in a poly-Asp helix), the only recourse for glycine is tertiary contacts, which means avoiding lipid-facing positions.

Of the 147 conserved glycines with |z| values of <10 Å in our benchmark set, 96 (65%) are found in close helix–helix contacts, meaning that these glycines are separated from the partner helix by no more than 110% of the minimal distance of a helix pair. Presumably, some of the other glycines could be in helix–helix contacts in alternative functional states of these proteins. In Figure 4a, we further show that, among the 26 benchmark proteins, 92 of the 220 helix–helix pairs that have heavy atom contacts with distances of <5 Å located in the hydrophobic region involve at least one glycine residue in these contacts. Furthermore, the results suggest that when glycine residues are involved the minimal distance between helices is somewhat decreased. Such a decrease in distance promotes not only additional van der Waals interactions but also potentially additional electrostatic interactions.

Glycine residues facilitate helix packing in a wide variety of ways (Figure 4b–f). Helices pack at different crossing angles. When the crossing angle is relatively small, various glycine motifs facilitate interactions over a considerable helical length (e.g., Figure 4d,e). When the crossing angle is larger, glycine residues also facilitate packing, sometimes with them on both helices (Figure 4f), but frequently on a single helix (Figure 4b,c). Glycines also facilitate helix kinking such as in Figure 4b, thereby increasing the helical contact. Without such a kink, the interactions between this pair of helices would be significantly reduced.

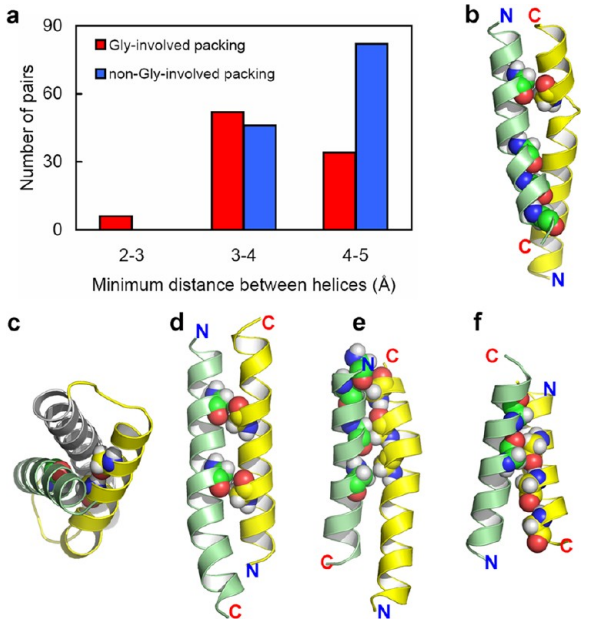

Figure 4. Involvement of glycines in helix packing. A total of 220 helix–helix pairs in the 26 benchmark proteins were identified. (a) Number of helix–helix pairs binned according to distance of the closest contact and grouped according to whether glycine is involved. (b–f) Examples of helix pairs showing helix packing facilitated by glycine residues, highlighted here in space-filling mode. (b) Helix 1 (yellow) residue 27 and helix 6 (green) residues 204, 211, 214, and 218 from PDB entry 2NS1. Gly27 and Gly211 both appear to induce kinks in the helix that facilitate helix–helix interactions along the entire length of the TM helices despite substantial crossing angles at both crossing points. (c) Helix 7 (gray), helix 8 (yellow) residues 264 and 268, and helix 9 (green) residue 288 from PDB entry 2NS1. (d) Helix 3 (yellow) residues 97 and 104 and helix 4 (green) residues 123 and 130 from PDB entry 3O7Q. The i to i + 7 glycine residues on both helices, along with a small crossing angle, result in a large van der Waals interaction surface. (e) Helix 11 (yellow) residues 402, 406, and 410 and helix 12 (green) residues 421, 424, and 428 from PDB entry 3MKT. Here a GxxxGxxxG motif interacts with a GxxGxxxG motif. (f) Helix 4 (yellow) residues 151, 155, and 159 and helix 5 (green) residues 176 and 180 from PDB entry 3ND0. Here a GxxxGxxxG motif interacts with a GxxxG motif.

SURFACE EXPOSURE OF GLYCINES

The forgoing results show that in native-like structures conserved glycine residues are primarily involved in enhancing helix–helix interactions and are not likely to be exposed to the lipid environment. The results led us to posit that the lack of exposure of conserved glycine residues to the fatty acyl chains of native membranes may be used as a criterion for assessing the native-like quality of membrane protein structures.

As a simple test of our glycine-based validation approach, we searched for exposed, conserved glycines in the three structures in Figure 1, which we already recognized as being non-native-like based on insufficient helix lengths, exposure of hydrophilic side chains, and a lack of oligomeric symmetry. Indeed, a number of conserved glycines are exposed in all these structures, including G444 located in helix 2 of KdpD (Figure 5a) and G435, G439, and G443 in TM helix 2 of ASIC (Figure 5b). A conserved glycine, G100, in helix 3 of FLAP was also

dx.doi.org/10.1021/bi300090x | Biochemistry 2012, 51, 4779–4789

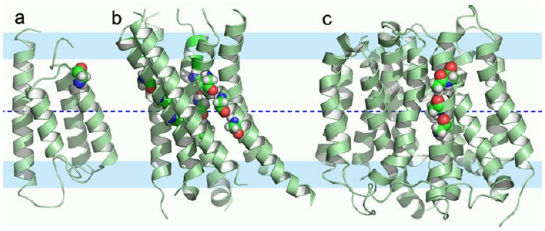

Figure 5. Application of the glycine-based validation tool. Conserved glycine residues that are exposed to the lipid interstices are highlighted in space-filling mode. (a) Gly444 from PDB entry 2KSF. (b) Glycine residues 435, 439, and 443 from each monomer of PDB entry 2QTS. (c) Glycine residues 333, 336, 340, and 341 of the multidrug transporter, EmrD (3.5 Å resolution structure, PDB entry 2GFP).

exposed as a result of the helix 3−helix 4 loop being drawn into the membrane interstices.

We also found exposed conserved glycines in the structure of EmrD (PDB entry 2GFP);[84] four conserved glycine residues, G333, G336, G340, and G341, in helix 11 are all exposed to the hydrophobic environment (Figure 5c), suggesting that there is a local packing problem. The loop between helices 11 and 12 contains only hydrophilic, not charged, residues, so the boundaries between the loop and these helices as well as the rotational orientation of these helices may be sensitive to a presumably weak hydrophobic environment in the crystal lattice. Indeed, several hydrophilic residues in these two helices are exposed (residues Gln343, Thr360, and Ser364), although both Gln343 and Thr360 are relatively close to the bilayer interfacial region. Consequently, these hydrophilic residues alone might not generate very much concern for this structure, while the exposed glycine residues generate a more significant concern. Other than the potential problem with helices 11 and 12, much of the rest of this large structure appears to be native-like. These results displayed in Figure 5 collectively support a need for validating whether a given membrane protein structure is compatible with the native membrane environment.

■ CONCLUDING REMARKS

A structural validation approach based on the exposure of conserved glycine residues has been suggested and supported through the development of a set of benchmark proteins representing approximately half of the helical membrane protein structure−function families and the identification of several distorted proteins having conserved glycine residues exposed to what would be the membrane interstices. The exposure of glycine to the lipid interstices is avoided in native-like structures, both to prevent exposing the helix backbone to the lipid hydrophobic environment and to allow for strengthened helix−helix packing. This validation approach was effective both in confirming putative non-native-like structures and in identifying a previously unrecognized non-native-like structure. Wide applicability is thus expected.

It should be recognized that, if a protein formed an oligomeric state or some other protein−protein complex, there might be a reason to have conserved glycine residues at the monomer−monomer interface. Many single-TM helical proteins have glycine residues, and we can expect that these proteins will either form oligomers or interact with other membrane proteins such that in complex the glycine residues will not be exposed. We would further anticipate that exposing conserved glycine residues to the membrane interstices should drive the binding reaction toward complex formation.[20] Interestingly, in the set of benchmark membrane proteins analyzed here, the monomeric units of oligomeric proteins appear to utilize conserved glycine residues only infrequently at the monomer−monomer interfaces, while alanine residues appear to be more common at these interfaces.

Given their destabilizing influence on water-soluble helices, how can the large number of glycine residues be tolerated in TM helices? These helices are primarily composed of aliphatic residues embedded in a low-dielectric environment that is largely devoid of water, leading to strengthened intrahelical hydrogen bonds.[21,23] Therefore, secondary structural stability is substantially increased in the membrane environment, and consequently, glycine residues can be tolerated at some cost to helical stability. However, the glycine residues facilitate helix−helix packing, allowing for strengthened electrostatic and van der Waals interactions between the helices. Therefore, the result of the increased level of glycine residues in TM helices is that excess secondary structural stability is sacrificed for increased tertiary structural stability, demonstrating an ingenious adaptation of membrane proteins to their environment.

Membrane protein structures are fundamentally important for many scientific communities, including those interested in understanding cellular physiology and the development of pharmaceuticals. Our inability to characterize protein structures in the native membrane environment leads to the use of membrane mimetics that may or may not be good models of the native environment for a given membrane protein. The validation approach described here can facilitate the verification of native-like structures and the recognition of non-native-like features that could otherwise mislead researchers who depend on the high fidelity of these important membrane protein structures.

■ ASSOCIATED CONTENT

Supporting Information

Details of how the structures from the PDB were processed and analyzed as well as reference helical structures, details for the calculation of solvent accessible surface areas and conservation scores, calculations for locating the center plane of the bilayer, and calculations for helix−helix contacts. This material is available free of charge via the Internet at http://pubs.acs.org.

■ AUTHOR INFORMATION

Corresponding Author

*E-mail: cross@magnet.fsu.edu. Telephone: (850) 644-0917. Fax: (850) 644-1366.

Funding

This research has been supported in part by National Institutes of Health Grants AI-074805 and GM-088187 and the National Science Foundation through Cooperative Agreement 0654118 between the Division of Materials Research and the State of Florida.

Notes

The authors declare no competing financial interest.

■ REFERENCES

(1) Tate, C. G. (2006) Comparison of three structures of the multidrug transporter EmrE. *Curr. Opin. Struct. Biol. 16*, 457−464.

(2) Cross, T. A., Sharma, M., Yi, M., and Zhou, H. X. (2011) Influence of solubilizing environments on membrane protein structures. *Trends Biochem. Sci. 36*, 117−125.

(3) Vinothkumar, K. R., and Henderson, R. (2010) Structures of membrane proteins. *Q. Rev. Biophys. 43*, 65−158.
(4) Verardi, R., Shi, L., Traaseth, N. J., Walsh, N., and Veglia, G. (2011) Structural topology of phospholamban pentamer in lipid bilayers by a hybrid solution and solid-state NMR method. *Proc. Natl. Acad. Sci. U.S.A. 108*, 9101−9106.
(5) Botelho, A. V., Huber, T., Sakmar, T. P., and Brown, M. F. (2006) Curvature and hydrophobic forces drive oligomerization and modulate activity of rhodopsin in membranes. *Biophys. J. 91*, 4464−4477.
(6) Botelho, A. V., Gibson, N. J., Thurmond, R. L., Wang, Y., and Brown, M. F. (2002) Conformational energetics of rhodopsin modulated by nonlamellar-forming lipids. *Biochemistry 41*, 6354−6368.
(7) Anfinsen, C. B. (1973) Principles that govern the folding of protein chains. *Science 181*, 223−230.
(8) Sanders, C. R., and Mittendorf, K. F. (2011) Tolerance to changes in membrane lipid composition as a selected trait of membrane proteins. *Biochemistry 50*, 7858−7867.
(9) Mitsuoka, K., Hirai, T., Murata, K., Miyazawa, A., Kidera, A., Kimura, Y., and Fujiyoshi, Y. (1999) The structure of bacteriorhodopsin at 3.0 Å resolution based on electron crystallography: Implication of the charge distribution. *J. Mol. Biol. 286*, 861−882.
(10) Sharma, M., Yi, M., Dong, H., Qin, H., Peterson, E., Busath, D. D., Zhou, H. X., and Cross, T. A. (2010) Insight into the mechanism of the influenza A proton channel from a structure in a lipid bilayer. *Science 330*, 509−512.
(11) Ketchem, R. R., Roux, B., and Cross, T. A. (1997) High-Resolution Polypeptide Structure in a Lamellar Phase Lipid Environment from Solid-State NMR Derived Orientational Constraints. *Structure 5*, 1655−1669.
(12) Das, B. B., Ajithkumar, T. G., Sinha, N., Opella, S. J., and Ramanathan, K. V. (2007) Cross- and axial-peak intensities in 2D-SLF experiments based on cross-polarization: The role of the initial density matrix. *J. Magn. Reson. 185*, 308−317.
(13) Park, S. H., Marassi, F. M., Black, D., and Opella, S. J. (2010) Structure and dynamics of the membrane-bound form of Pf1 coat protein: Implications of structural rearrangement for virus assembly. *Biophys. J. 99*, 1465−1474.
(14) Park, S. H., De Angelis, A. A., Nevzorov, A. A., Wu, C. H., and Opella, S. J. (2006) Three-dimensional structure of the transmembrane domain of Vpu from HIV-1 in aligned phospholipid bicelles. *Biophys. J. 91*, 3032−3042.
(15) Grigorieff, N., Ceska, T. A., Downing, K. H., Baldwin, J. M., and Henderson, R. (1996) Electron crystallographic refinement of the structure of bacteriorhodopsin. *J. Mol. Biol. 259*, 393−421.
(16) Gonen, T., Cheng, Y., Sliz, P., Hiroaki, Y., Fujiyoshi, Y., Harrison, S. C., and Walz, T. (2005) Lipid-protein interactions in double-layered two-dimensional AQP0 crystals. *Nature 438*, 633−638.
(17) Hite, R. K., Gonen, T., Harrison, S. C., and Walz, T. (2008) Interactions of lipids with aquaporin-0 and other membrane proteins. *Pfluegers Arch. 456*, 651−661.
(18) Popot, J. L., and Engelman, D. M. (2000) Helical Membrane Protein Folding, Stability and Evolution. *Annu. Rev. Biochem. 69*, 881−922.
(19) Hu, J., Asbury, T., Achuthan, S., Li, C., Bertram, R., Quine, J. R., Fu, R., and Cross, T. A. (2007) Backbone structure of the amantadine-blocked trans-membrane domain M2 proton channel from influenza A virus. *Biophys. J. 92*, 4335−4343.
(20) MacKenzie, K. R., and Fleming, K. G. (2008) Association energetics of membrane spanning α-helices. *Curr. Opin. Struct. Biol. 18*, 412−419.
(21) Kim, S., and Cross, T. A. (2002) Uniformity, ideality, and hydrogen bonds in transmembrane α-helices. *Biophys. J. 83*, 2084−2095.
(22) Page, R. C., Li, C., Hu, J., Gao, F. P., and Cross, T. A. (2007) Lipid bilayers: An essential environment for the understanding of membrane proteins. *Magn. Reson. Chem. 45*, S2−S11.
(23) Page, R. C., Kim, S., and Cross, T. A. (2008) Transmembrane helix uniformity examined by spectral mapping of torsion angles. *Structure 16*, 787−797.
(24) Eilers, M., Patel, A. B., Liu, W., and Smith, S. O. (2002) Comparison of helix interactions in membrane and soluble α-bundle proteins. *Biophys. J. 82*, 2720−2736.
(25) Dutzler, R., Campbell, E. B., and MacKinnon, R. (2003) Gating the selectivity filter in ClC chloride channels. *Science 300*, 108−112.
(26) Jiang, Y., Lee, A., Chen, J., Ruta, V., Cadene, M., Chait, B. T., and MacKinnon, R. (2003) X-ray structure of a voltage-dependent K^+ channel. *Nature 423*, 33−41.
(27) Cherezov, V., Rosenbaum, D. M., Hanson, M. A., Rasmussen, S. G., Thian, F. S., Kobilka, T. S., Choi, H. J., Kuhn, P., Weis, W. I., Kobilka, B. K., and Stevens, R. C. (2007) High-resolution crystal structure of an engineered human β2-adrenergic G protein-coupled receptor. *Science 318*, 1258−1265.
(28) Serrano-Vega, M. J., Magnani, F., Shibata, Y., and Tate, C. G. (2008) Conformational thermostabilization of the β1-adrenergic receptor in a detergent-resistant form. *Proc. Natl. Acad. Sci. U.S.A. 105*, 877−882.
(29) Butterwick, J. A., and MacKinnon, R. (2010) Solution structure and phospholipid interactions of the isolated voltage-sensor domain from KvAP. *J. Mol. Biol. 403*, 591−606.
(30) Lee, S. Y., Lee, A., Chen, J., and MacKinnon, R. (2005) Structure of the KvAP voltage-dependent K^+ channel and its dependence on the lipid membrane. *Proc. Natl. Acad. Sci. U.S.A. 102*, 15441−15446.
(31) Vargas, E., Bezanilla, F., and Roux, B. (2011) In search of a consensus model of the resting state of a voltage-sensing domain. *Neuron 72*, 713−720.
(32) Rosenberg, M. F., O'Ryan, L. P., Hughes, G., Zhao, Z., Aleksandrov, L. A., Riordan, J. R., and Ford, R. C. (2011) The cystic fibrosis transmembrane conductance regulator (CFTR): Three-dimensional structure and localization of a channel gate. *J. Biol. Chem. 286*, 42647−42654.
(33) Abe, K., Tani, K., and Fujiyoshi, Y. (2011) Conformational rearrangement of gastric H^+,K^+-ATPase induced by an acid suppressant. *Nat. Commun. 2*, 155.
(34) Oshima, A., Tani, K., Toloue, M. M., Hiroaki, Y., Smock, A., Inukai, S., Cone, A., Nicholson, B. J., Sosinsky, G. E., and Fujiyoshi, Y. (2011) Asymmetric configurations and N-terminal rearrangements in connexin26 gap junction channels. *J. Mol. Biol. 405*, 724−735.
(35) Fleishman, S. J., Harrington, S. E., Enosh, A., Halperin, D., Tate, C. G., and Ben-Tal, N. (2006) Quasi-symmetry in the cryo-EM structure of EmrE provides the key to modeling its transmembrane domain. *J. Mol. Biol. 364*, 54−67.
(36) Hessa, T., White, S. H., and von Heijne, G. (2005) Membrane insertion of a potassium-channel voltage sensor. *Science 307*, 1427.
(37) Bond, P. J., Wee, C. L., and Sansom, M. S. (2008) Coarse-grained molecular dynamics simulations of the energetics of helix insertion into a lipid bilayer. *Biochemistry 47*, 11321−11331.
(38) Gray, T. M., and Matthews, B. W. (1984) Intrahelical hydrogen bonding of serine, threonine and cysteine residues within α-helices and its relevance to membrane-bound proteins. *J. Mol. Biol. 175*, 75−81.
(39) Adamian, L., Nanda, V., DeGrado, W. F., and Liang, J. (2005) Empirical lipid propensities of amino acid residues in multispan α helical membrane proteins. *Proteins 59*, 496−509.
(40) Parton, D. L., Klingelhoefer, J. W., and Sansom, M. S. (2011) Aggregation of model membrane proteins, modulated by hydrophobic mismatch, membrane curvature, and protein class. *Biophys. J. 101*, 691−699.
(41) Schafer, L. V., de Jong, D. H., Holt, A., Rzepiela, A. J., de Vries, A. H., Poolman, B., Killian, J. A., and Marrink, S. J. (2011) Lipid packing drives the segregation of transmembrane helices into disordered lipid domains in model membranes. *Proc. Natl. Acad. Sci. U.S.A. 108*, 1343−1348.
(42) de Planque, M. R., Greathouse, D. V., Koeppe, R. E., II, Schafer, H., Marsh, D., and Killian, J. A. (1998) Influence of lipid/peptide hydrophobic mismatch on the thickness of diacylphosphatidylcholine

bilayers. A ^{2}H NMR and ESR study using designed transmembrane α-helical peptides and gramicidin A. *Biochemistry 37*, 9333−9345.
(43) Engelman, D. M. (2005) Membranes are more mosaic than fluid. *Nature 438*, 578−580.
(44) Phillips, R., Ursell, T., Wiggins, P., and Sens, P. (2009) Emerging roles for lipids in shaping membrane-protein function. *Nature 459*, 379−385.
(45) Cantor, R. S. (1999) Lipid composition and the lateral pressure profile in bilayers. *Biophys. J. 76*, 2625−2639.
(46) Chou, J. J., Kaufman, J. D., Stahl, S. J., Wingfield, P. T., and Bax, A. (2002) Micelle-Induced Curvature in a Water-Insoluble HIV-1 Env Peptide Revealed by NMR Dipolar Coupling Measurement in Stretched Polyacrylamide Gel. *J. Am. Chem. Soc. 124*, 2450−2451.
(47) Kalyanasundaram, K., and Thomas, J. K. (1977) Environmental Effects on Vibronic Band Intensities in Pyrene Monomer Flourescence and Their Application in Studies of Micellar Systems. *J. Am. Chem. Soc. 99*, 2039−2044.
(48) Fendler, J. H., and Fendler, E. J. (1975) *Catalysis in Micellar and Macromolecular Systems*, Academic Press, New York.
(49) Podo, F., Ray, A., and Nemethy, G. (1973) Structure and Hydration of Nonionic Detergent Micelles. High Resolution Nucelar Magnetic Resonance Study. *J. Am. Chem. Soc. 95*, 6164−6171.
(50) Landau, E. M., and Rosenbusch, J. P. (1996) Lipidic cubic phases: A novel concept for the crystallization of membrane proteins. *Proc. Natl. Acad. Sci. U.S.A. 93*, 14532−14535.
(51) Cevc, G., and Marsh, D. (1987) *Phospholipid Bilayers: Physical Principles and Models*, Vol. *5*, John Wiley & Sons, New York.
(52) Higman, V. A., Varga, K., Aslimovska, L., Judge, P. J., Sperling, L. J., Rienstra, C. M., and Watts, A. (2011) The Conformation of Bacteriorhodopsin Loops in Purple Membranes Resolved by Solid-State MAS NMR Spectroscopy. *Angew. Chem., Int. Ed. 50*, 8432−8435.
(53) Maslennikov, I., Klammt, C., Hwang, E., Kefala, G., Okamura, M., Esquivies, L., Mors, K., Glaubitz, C., Kwiatkowski, W., Jeon, Y. H., and Choe, S. (2010) Membrane domain structures of three classes of histidine kinase receptors by cell-free expression and rapid NMR analysis. *Proc. Natl. Acad. Sci. U.S.A. 107*, 10902−10907.
(54) Ferguson, A. D., McKeever, B. M., Xu, S., Wisniewski, D., Miller, D. K., Yamin, T. T., Spencer, R. H., Chu, L., Ujjainwalla, F., Cunningham, B. R., Evans, J. F., and Becker, J. W. (2007) Crystal structure of inhibitor-bound human 5-lipoxygenase-activating protein. *Science 317*, 510−512.
(55) Jegerschold, C., Pawelzik, S. C., Purhonen, P., Bhakat, P., Gheorghe, K. R., Gyobu, N., Mitsuoka, K., Morgenstern, R., Jakobsson, P. J., and Hebert, H. (2008) Structural basis for induced formation of the inflammatory mediator prostaglandin E2. *Proc. Natl. Acad. Sci. U.S.A. 105*, 11110−11115.
(56) Jasti, J., Furukawa, H., Gonzales, E. B., and Gouaux, E. (2007) Structure of acid-sensing ion channel 1 at 1.9 Å resolution and low pH. *Nature 449*, 316−323.
(57) Gonzales, E. B., Kawate, T., and Gouaux, E. (2009) Pore architecture and ion sites in acid-sensing ion channels and P2X receptors. *Nature 460*, 599−604.
(58) von Heijne, G. (1981) Membrane proteins: The amino acid composition of membrane-penetrating segments. *Eur. J. Biochem. 120*, 275−278.
(59) O'Neil, K. T., and DeGrado, W. F. (1990) A thermodynamic scale for the helix-forming tendencies of the commonly occurring amino acids. *Science 250*, 646−651.
(60) Lyu, P. C., Liff, M. I., Marky, L. A., and Kallenbach, N. R. (1990) Side chain contributions to the stability of α-helical structure in peptides. *Science 250*, 669−673.
(61) Pace, C. N., and Scholtz, J. M. (1998) A helix propensity scale based on experimental studies of peptides and proteins. *Biophys. J. 75*, 422−427.
(62) Chou, P. Y., and Fasman, G. D. (1974) Conformational parameters for amino acids in helical, β-sheet, and random coil regions calculated from proteins. *Biochemistry 13*, 211−222.
(63) Senes, A., Ubarretxena-Belandia, I., and Engelman, D. M. (2001) The Cα−H···O hydrogen bond: A determinant of stability and specificity in transmembrane helix interactions. *Proc. Natl. Acad. Sci. U.S.A. 98*, 9056−9061.
(64) Grottesi, A., Domene, C., Hall, B., and Sansom, M. S. (2005) Conformational dynamics of M2 helices in KirBac channels: Helix flexibility in relation to gating via molecular dynamics simulations. *Biochemistry 44*, 14586−14594.
(65) Yi, M., Cross, T. A., and Zhou, H. X. (2009) Conformational heterogeneity of the M2 proton channel and a structural model for channel activation. *Proc. Natl. Acad. Sci. U.S.A. 106*, 13311−13316.
(66) Doyle, D. A., Cabral, J. M., Pfuetzner, R. A., Kuo, A., Gulbis, J. M., Cohen, S. L., Chait, B. T., and MacKinnon, R. (1998) The Structure of the Potassium Channel: Molecular Basis of K^+ Conduction and Selectivity. *Science 280*, 69−77.
(67) Xu, F., Wang, A., Vaughn, J. B., Jr., and Cross, T. A. (1996) A Catalytic Role for Protic Solvents in Conformational Interconversion. *J. Am. Chem. Soc. 118*, 9176−9177.
(68) Xu, F., and Cross, T. A. (1999) Water: Foldase activity in catalyzing polypeptide conformational rearrangements. *Proc. Natl. Acad. Sci. U.S.A. 96*, 9057−9061.
(69) Brewer, M. L., Schmitt, U. W., and Voth, G. A. (2001) The formation and dynamics of proton wires in channel environments. *Biophys. J. 80*, 1691−1702.
(70) Pomès, R., and Roux, B. (1996) Structure and dynamics of a proton wire: A theoretical study of H^+ translocation along the single-file water chain in the gramicidin A channel. *Biophys. J. 71*, 19−39.
(71) Javadpour, M. M., Eilers, M., Groesbeek, M., and Smith, S. O. (1999) Helix packing in polytopic membrane proteins: Role of glycine in transmembrane helix association. *Biophys. J. 77*, 1609−1618.
(72) MacKenzie, K. R., Prestegard, J. H., and Engelman, D. M. (1997) A Transmembrane Helix Dimer: Structure and Implications. *Science 276*, 131−133.
(73) Yohannan, S., Faham, S., Yang, D., Grosfeld, D., Chamberlain, A. K., and Bowie, J. U. (2004) A Cα-H···O hydrogen bond in a membrane protein is not stabilizing. *J. Am. Chem. Soc. 126*, 2284−2285.
(74) Russ, W. P., and Engelman, D. M. (2000) The GxxxG motif: A framework for transmembrane helix-helix association. *J. Mol. Biol. 296*, 911−919.
(75) Melnyk, R. A., Kim, S., Curran, A. R., Engelman, D. M., Bowie, J. U., and Deber, C. M. (2004) The affinity of GXXXG motifs in transmembrane helix-helix interactions is modulated by long-range communication. *J. Biol. Chem. 279*, 16591−16597.
(76) Kleiger, G., Grothe, R., Mallick, P., and Eisenberg, D. (2002) GXXXG and AXXXA: Common α-helical interaction motifs in proteins, particularly in extremophiles. *Biochemistry 41*, 5990−5997.
(77) Senes, A., Engel, D. E., and DeGrado, W. F. (2004) Folding of helical membrane proteins: The role of polar, GxxxG-like and proline motifs. *Curr. Opin. Struct. Biol. 14*, 465−479.
(78) Kim, S., Jeon, T. J., Oberai, A., Yang, D., Schmidt, J. J., and Bowie, J. U. (2005) Transmembrane glycine zippers: Physiological and pathological roles in membrane proteins. *Proc. Natl. Acad. Sci. U.S.A. 102*, 14278−14283.
(79) Wigley, W. C., Corboy, M. J., Cutler, T. D., Thibodeau, P. H., Oldan, J., Lee, M. G., Rizo, J., Hunt, J. F., and Thomas, P. J. (2002) A protein sequence that can encode native structure by disfavoring alternate conformations. *Nat. Struct. Biol. 9*, 381−388.
(80) Deber, C. M., and Therien, A. G. (2002) Putting the β-breaks on membrane protein misfolding. *Nat. Struct. Biol. 9*, 318−319.
(81) Rodrigues, M. L., Oliveira, T. F., Pereira, I. A., and Archer, M. (2006) X-ray structure of the membrane-bound cytochrome c quinol dehydrogenase NrfH reveals novel haem coordination. *EMBO J. 25*, 5951−5960.
(82) Jayaram, H., Robertson, J. L., Wu, F., Williams, C., and Miller, C. (2011) Structure of a slow CLC Cl/H^+ antiporter from a cyanobacterium. *Biochemistry 50*, 788−794.
(83) Ashkenazy, H., Erez, E., Martz, E., Pupko, T., and Ben-Tal, N. (2010) ConSurf 2010: Calculating evolutionary conservation in sequence and structure of proteins and nucleic acids. *Nucleic Acids Res. 38*, W529−W533.

(84) Yin, Y., He, X., Szewczyk, P., Nguyen, T., and Chang, G. (2006) Structure of the multidrug transporter EmrD from *Escherichia coli*. *Science 312*, 741−744.